1st International Symposium on Laser Ultrasonics: Science, Technology and Applications
July 16-18 2008, Montreal, Canada

# Acoustic Waves Generated by a Laser Line Source on the Surface of a Cylindrical Rod or Cavity

Yongdong PAN [1], Nikolay CHIGAREV [2], Clement ROSSIGNOL [2], Bertrand AUDOIN [2]

[1] Institute of Acoustics, Tongji University(*1239 siping road* ), Shanghai, 200092, China; Phone: +86 21 6598 3797, Fax +86 21 6598 3797; email: ypan@mail.tongji.edu.cn
[2] Laboratoire de Mécanique Physique, Université Bordeaux 1, Talence, 33405, France; email : n.chigarev@lmp.u-bordeaux1.fr, c.rossignol@lmp.u-bordeaux1.fr, b.audoin@lmp.u-bordeaux1.fr

**Abstract**
In this work, a model is proposed to predict acoustic waves generated in a homogeneous and isotropic cylindrical cavity by a laser line source. The Fourier series expansion is introduced for one spatial coordinate to solve this transient response problem. Theoretical displacements are obtained for an aluminum cylindrical cavity of internal diameter 40 mm. The corresponding displacements are observed experimentally by the laser ultrasonic technique. For comparison, theoretical and experimental waveforms are also provided for an aluminium cylindrical rod under laser line source excitation. Good agreement is found in the time arrival, shape and relative amplitude of surface acoustic waves. The dispersion of surface acoustic waves is quite different to that on a cylindrical rod.
**Keywords:** Laser ultrasound, cylindrical cavity, surface acoustic wave, cylindrical rod

## 1. Introduction

Cylindrical cavity structures are extensively applied in industries, it requires the understanding of the transient wave propagation along the circumferential direction for a nondestructive evaluation purpose, such as a concrete tunnel inspection. With such an unique geometry, the corresponding acoustic wave propagation is an important issue for research. Although the surface acoustic wave on cylindrical rod and cavity has been studied in detail by Viktorov [1] in 1967, few experimental results were published due to the coupling difficulty of the conventional piezoelectric transducer method. With the advantages of the laser ultrasonic technique [2], the surface acoustic wave on a sphere was first observed experimentally in 1988 [3], and a further detailed study has been reported recently [4]. Even though recent studies [5-8] have been carried out on cylindrical structures using the same technique, the propagation of the acoustic waves generated by a laser line pulse is still not clearly understood. In this paper, a theoretical solution is presented to predict the acoustic field generated by the laser line pulse in either ablation or thermoelastic regime for a homogenous and isotropic cylindrical cavity. Calculated waveforms of the normal displacement component are compared with experimental signals captured by the laser ultrasonic technique.

## 2. General formulation

Consider a homogenous and isotropic cylindrical cavity of infinite length, radius $a$, and density $\rho$, with its axis of symmetry coinciding with the $z$-axis of its cylindrical coordinates ($r$, $\theta$, $z$). Let $\lambda$ and $\mu$ denote the two independent elastic constants related to the isotropic plane perpendicular to the $z$-axis. The laser line source lies at the boundary

$r=a$, and it is orientated along the $z$ direction. Owing to the symmetry, this problem shows invariance along $z$ direction. The non-zero components $u_r$ and $u_\theta$ of the displacement vector depend on two spatial variables $r$, $\theta$ and on time $t$. They can be written as [7]

$$\begin{cases} u_r(r,\theta,t) = \dfrac{\partial \varphi}{\partial r} + \dfrac{1}{r}\dfrac{\partial \psi}{\partial \theta} \\ u_\theta(r,\theta,t) = \dfrac{1}{r}\dfrac{\partial \varphi}{\partial \theta} - \dfrac{\partial \psi}{\partial r} \end{cases} \tag{1}$$

where the two scalar potentials $\varphi$ and $\psi$ are governed by the wave motion equations

$$\begin{cases} \dfrac{\partial^2 \varphi}{\partial r^2} + \dfrac{1}{r}\dfrac{\partial \varphi}{\partial r} + \dfrac{1}{r^2}\dfrac{\partial^2 \varphi}{\partial \theta^2} = \dfrac{\rho}{\lambda+2\mu}\dfrac{\partial^2 \varphi}{\partial t^2} \\ \dfrac{\partial^2 \psi}{\partial r^2} + \dfrac{1}{r}\dfrac{\partial \psi}{\partial r} + \dfrac{1}{r^2}\dfrac{\partial^2 \psi}{\partial \theta^2} = \dfrac{\rho}{\mu}\dfrac{\partial^2 \psi}{\partial t^2} \end{cases} \tag{2}$$

and by either of the following boundary conditions. For a source at position $\theta$=0°, two components $\sigma_{rr}$ and $\sigma_{r\theta}$ of the stress tensor at any point of the surface are determined by either

$$\begin{cases} \sigma_{rr}\big|_{r=a} = -F_0\delta(t)\delta(\theta) \\ \sigma_{r\theta}\big|_{r=a} = 0 \end{cases} \tag{3}$$

for the ablation regime [2], or

$$\begin{cases} \sigma_{rr}\big|_{r=a} = 0 \\ \sigma_{r\theta}\big|_{r=a} = -F_0 h(t)\delta'(\theta) \end{cases} \tag{4}$$

for the thermoelastic regime [2]. In Eqs. (3) and (4), $F_0$ is a certain loading in N·μs·m$^{-1}$ related to the laser line pulse. Here a delta function of time $\delta(t)$ and a Heaviside step function of time $h(t)$ are used for the ablation and thermoelastic generations, respectively; and $\delta'(\theta)$ denotes the derivative of the delta function $\delta(\theta)$. In Eq. (3), a delta force is postulated in time and space to represent sudden normal loading in the ablation regime. A Heaviside step function in time is considered in the thermoelastic regime [Eq. (4)] since thermal diffusion is neglected.

## 3. Transformed solution and numerical inversion scheme

The two-dimensional Fourier transform of the displacement field over the coordinate $\theta$ and time $t$ is now considered as follows

$$U_i(r,\nu,\omega) = \int_{-\infty}^{+\infty}\int_{-\infty}^{+\infty} u_i(r,\theta,t)e^{j(\nu\theta-\omega t)}dtd\theta \qquad (i=r \text{ or } \theta) \tag{5}$$

with $\nu=k_\theta a$, and $k_\theta$ is the component of the wave vector $\boldsymbol{k}$ along $\theta$ direction. Doing so, the partially derivative equation Eq. (2) becomes linear, providing explicit solution forms for the potentials $\varphi$ and $\psi$. The displacement components are then obtained for ablation regime

$$\begin{cases} U_r(r,\nu,\omega) = -\dfrac{F_0 a}{2\mu D_\nu}\left\{\left(\nu^2 - \dfrac{k_{\mathrm{T}}^2 a^2}{2} - B_{\mathrm{T}}\right) B_{\mathrm{L}} \dfrac{Y_\nu'(k_{\mathrm{L}} r)}{Y_\nu'(k_{\mathrm{L}} a)} + \nu^2 (1-B_{\mathrm{L}}) \dfrac{a}{r} \dfrac{Y_\nu(k_{\mathrm{T}} r)}{Y_\nu(k_{\mathrm{T}} a)}\right\} \\ U_\theta(r,\nu,\omega) = \dfrac{j\nu F_0 a}{2\mu D_\nu}\left\{\left(\nu^2 - \dfrac{k_{\mathrm{T}}^2 a^2}{2} - B_{\mathrm{T}}\right) \dfrac{a}{r} \dfrac{Y_\nu(k_{\mathrm{L}} r)}{Y_\nu(k_{\mathrm{L}} a)} + (1-B_{\mathrm{L}}) B_{\mathrm{T}} \dfrac{Y_\nu'(k_{\mathrm{T}} r)}{Y_\nu'(k_{\mathrm{T}} a)}\right\} \end{cases} \tag{6}$$

and for thermoelastic regime

$$\begin{cases} U_r(r,\nu,\omega) = -\dfrac{\nu^2 F_0 a H(\omega)}{2\mu D_\nu}\left\{(1-B_{\mathrm{T}}) B_{\mathrm{L}} \dfrac{Y_\nu'(k_{\mathrm{L}} r)}{Y_\nu'(k_{\mathrm{L}} a)} + \left(\nu^2 - \dfrac{k_{\mathrm{T}}^2 a^2}{2} - B_{\mathrm{L}}\right) \dfrac{a}{r} \dfrac{Y_\nu(k_{\mathrm{T}} r)}{Y_\nu(k_{\mathrm{T}} a)}\right\} \\ U_\theta(r,\nu,\omega) = \dfrac{j\nu F_0 a H(\omega)}{2\mu D_\nu}\left\{\nu^2 (1-B_{\mathrm{T}}) \dfrac{a}{r} \dfrac{Y_\nu(k_{\mathrm{L}} r)}{Y_\nu(k_{\mathrm{L}} a)} + \left(\nu^2 - \dfrac{k_{\mathrm{T}}^2 a^2}{2} - B_{\mathrm{L}}\right) B_{\mathrm{T}} \dfrac{Y_\nu'(k_{\mathrm{T}} r)}{Y_\nu'(k_{\mathrm{T}} a)}\right\} \end{cases} \tag{7}$$

where

$$\begin{cases} D_\nu = \left(\nu^2 - k_{\mathrm{T}}^2 a^2/2\right)^2 - \nu^2 + k_{\mathrm{T}}^2 a^2 \left(B_{\mathrm{L}} + B_{\mathrm{T}}\right)/2 + \left(1-\nu^2\right) B_{\mathrm{L}} B_{\mathrm{T}} \\ B_{\mathrm{L}} = k_{\mathrm{L}} a Y_\nu'\left(k_{\mathrm{L}} a\right) / Y_\nu\left(k_{\mathrm{L}} a\right), \\ B_{\mathrm{T}} = k_{\mathrm{T}} a Y_\nu'\left(k_{\mathrm{T}} a\right) / Y_\nu\left(k_{\mathrm{T}} a\right). \end{cases} \tag{8}$$

In Eqs. (6)-(8), $k_{\mathrm{L}} = \omega\sqrt{\rho/(\lambda+2\mu)}$ and $k_{\mathrm{T}} = \omega\sqrt{\rho/\mu}$ are the scalar wave vector of the longitudinal and transverse waves, respectively. And, $H(\omega)$ is the Fourier transform of Heaviside step function $h(t)$, and $Y_\nu'(x)$ is the derivative of Bessel function $Y_\nu(x)$. The corresponding solutions for a cylindrical rod can be obtained by replacing the Bessel function of the second kind $Y_\nu(x)$ by the Bessel function of the first kind $J_\nu(x)$ [7].

Now, let us focus on the numerical inversion scheme. When dealing with an elastic material, the solutions in Eqs. (6)-(7) show discontinuities for particular $k_\theta$ values. They correspond to poles associated with the zeros of the dispersion equation

$$D_\nu = 0\,. \tag{9}$$

For a rod instead of a cavity, the dispersion curves describe the cylindrical Rayleigh waves and Whispering Gallery waves [1]. Therefore, the inversion appears to be not consistent with the Fourier transformation. A suited numerical integration method should be applied. For each value of the angular frequency $\omega$, the integral on the real axis of the variable $k_\theta$ is calculated by the method suggested by Weaver et al [9]. In this scheme, the Fourier transform is generalized by replacing $\omega$ by a complex variable $\omega$-$j\delta$ with a small, constant and imaginary part $\delta$. With this change of variable, the inversion of Eq. (5) becomes

$$u_i(r,\theta,t) = (2\pi)^{-2} e^{\delta t} \int_{-\infty}^{+\infty} \left( \sum_{-\infty}^{+\infty} U_i(r,\nu,\omega) e^{-j\nu\theta} \right) e^{j\omega t} d\omega \tag{10}$$

The benefit of this inversion scheme is twofold: (i) it preserves the application of the fast Fourier transform algorithms for the final inversion, and (ii) the integrand is a nonsingular function that may now be integrated numerically.

## 4. Result on a cylindrical rod

The transient displacement can be calculated for either regime at the surface of aluminum cylindrical rods, and the value $\delta$=0.06 rad·μs$^{-1}$ was chosen. They are compared to corresponding experimental waveforms. A Nd:YAG laser was used for ultrasonic wave generation in either ablation or thermoelastic regime. The pulse duration is 10 ns and infrared light emission is 1064 nm with maximum burst energy of 340 mJ. The collimated optical beam was focused by a cylindrical lens. The line length and width are about 6 cm and 0.1 mm, respectively. An optical heterodyne probe with a power of 100 mW and a sensitivity [3] of $10^{-14}$ m/$\sqrt{\text{Hz}}$, was applied to measure the laser excited displacement.

The experimental and calculated displacements are shown in Fig. 1(a) for ablation regime (2*a*=9.97 mm) and Fig. 1(b) for thermoelastic regime (2*a*=4.12 mm), for an observation angle of 180°. Both waveforms are in good agreement for both regimes. The time, shape and relative amplitude of each arrival are identical. The arrival of the cylindrical Rayleigh wave (*R*) and its dispersive behavior (the component of the low frequency part travels relatively fast) are clearly observed for both waveforms. The direct longitudinal wave (*L*) and the reflected transverse wave (*TT*) are observed under the ablation regime, whereas they are not observable under the thermoelastic regime. This phenomenon can be explained by the different directivities of both regimes.[2] Moreover, the difference of the directivity can also explain the difference in relative amplitude of the reflected longitudinal waves (*LL*) and the head waves (*HW*) between both regimes. The corresponding arrivals of these bulk waves emphasize the good agreement between experiment and theory.

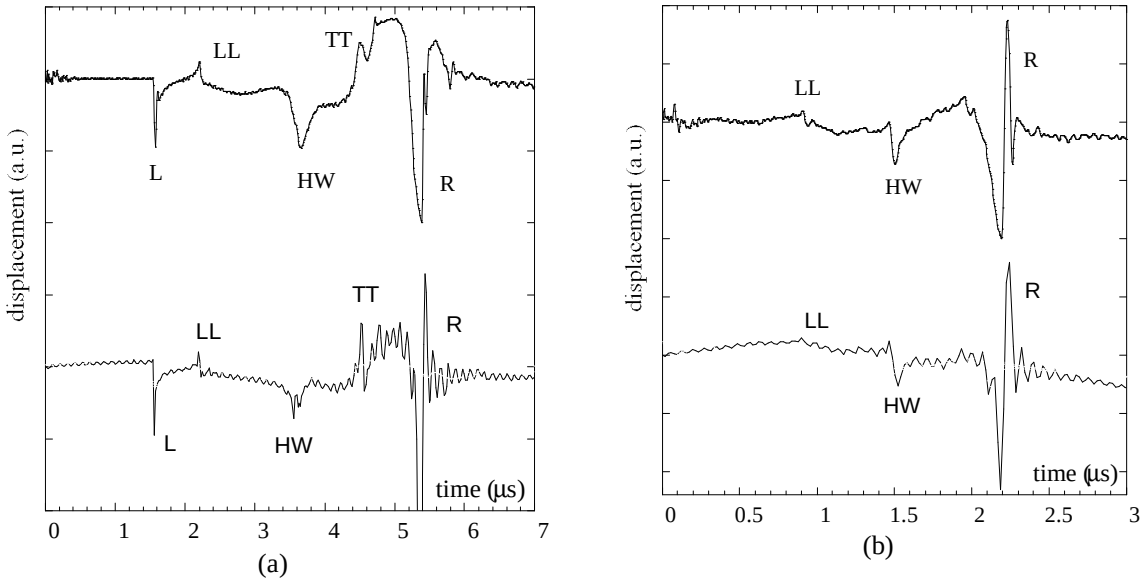


Figure 1. Experimental (top) and calculated (below) displacements at an observation angle of 180° for an aluminum cylindrical rod under (a) ablation regime (b) thermoelastic regime.

## 5. Result on a cylindrical cavity

To emphasize the difference between cylindrical cavity and rod, dispersion spectrums are calculated for both structures. They are made of aluminium and the diameter is 10 mm. As shown in Fig. 2(a) and (b), the dispersion of various wave modes are clearly observable for both structures. They are Rayleigh (*R*) and various orders of Whishpering Gallery (W1,W2,…) waves [1]. The spectrum is in good agreement with the dispersion curves (white dash lines in Fig. 2(a)) calculated through dispersion equation for cylindrical rod. The dispersion of Rayleigh wave is quite different between both structures, it is close to a straight line for cavity instead of a curved line for rod. This indicates the structure difference.

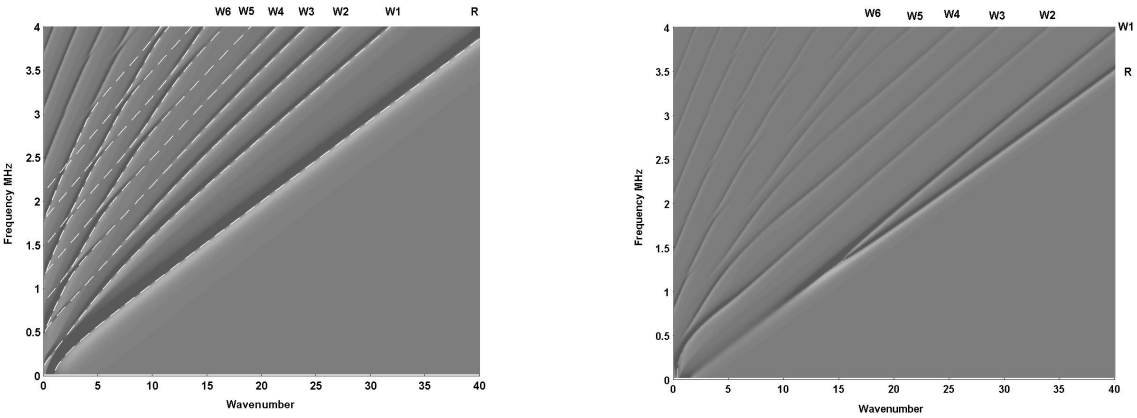


(a) (b)

Figure 2. Dispersion spectrums for (a) cylindrical rod and (b) cylindrical cavity.

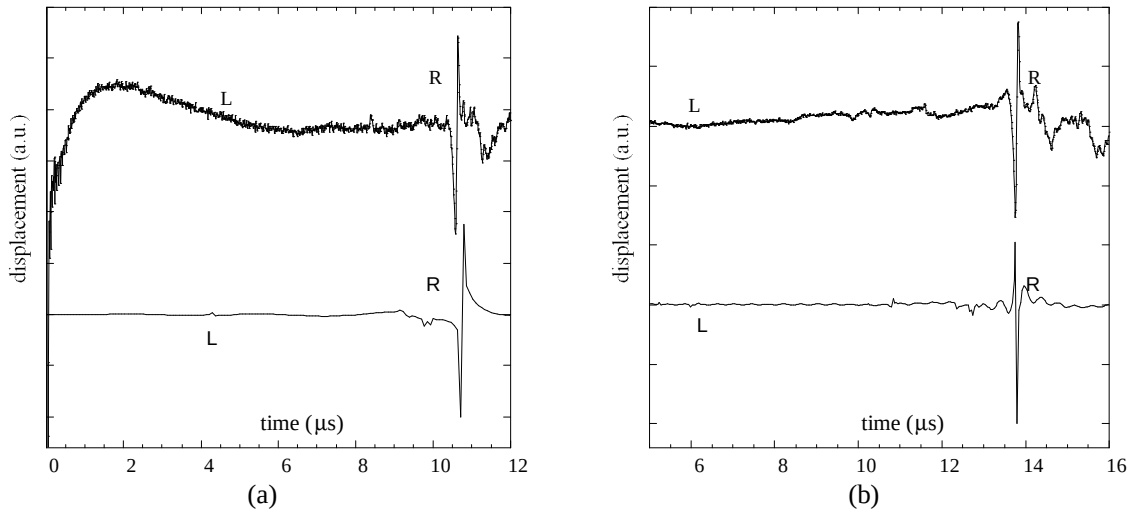


(a) (b)

Figure 3. Experimental (top) and calculated (below) displacements for an aluminum cylindrical cavity at an observation angle of (a) 90° (b) 115°.

The transient displacement for a cylindrical cavity can also be calculated and compared to experiment. The same $\delta$ value was chosen and the same experimental technique was

applied to measure the laser excited displacement. As shown in Fig. 3, the experimental and calculated waveforms are in good agreement at an observation angle of (a) 90° (b) 115° for an aluminum cavity of size 40mm in diameter. The arrival of the cylindrical Rayleigh wave (*R*) are clearly observed for both cases, and the arrival time, shape and relative amplitude are almost identical. The Rayleigh wave dispersion is quite different to that for a cylindrical rod, here no low frequency component travels faster than the high frequency component. The experimental signal from 0-5μs is the direct interference of the laser source to the interferometer for this one-side generation and detection.

## 5. Conclusions

A theoretical solution has been presented to predict the acoustic field generated by a laser line pulse in homogeneous and isotropic cylindrical cavity. Experimental and theoretical displacements for either an aluminum cylindrical rod or cavity are obtained and compared. Good agreements are observed in the time, shape and relative amplitude of the cylindrical Rayleigh waves. These results will be helpful in identifying the useful wave modes when dealing with the inverse problem of the nondestructive evaluation of cylindrical parts.

**Acknowledgements**

Y.P. was supported by CNRS under PICS No. 3357 and by the Natural Science Foundation of China under Grant No. 10432030. He is grateful to the hospitality of Laboratoire de Mécanique Physique, Université Bordeaux 1, France.

**References**

1. A. Viktorov, *Rayleigh and Lamb Waves*, Plenum Press, New York, 1967.
2. C. B. Scruby and L. E. Drain, *Laser Ultrasonics : Techniques and Applications*, Adam Hilger, New York, 1990.
3. D. Royer, E. Dieulesaint, X. Jia, and Y. Shui, 'Optical generation and detection of surface acoustic waves on a sphere,' *Appl. Phys. Lett.*, **52**, pp 706-708, 1988.
4. S. Ishikawa, H. Cho, Y. Tsukahara, N. Nakaso, and K. Yamanaka, 'Analysis of spurious bulk waves in ball surface wave device,' *Ultrasonics*, **41**, pp 1-8, 2003.
5. D. Clorennec and D. Royer, 'Analysis of surface acoustic wave propagation on a cylinder using laser ultrasonics,' *Appl. Phys. Lett.*, **82**, pp 4608-4610, 2003.
6. X. Wu, M. Qian, J-H Cantrell, 'Dispersive properties of cylindrical waves,' *Appl. Phys. Lett.*, **83**, pp 4053-4055, 2003.
7. Y. Pan, C. Rossignol, and B. Audoin, 'Acoustic waves generated by a laser line pulse in a transversely isotropic cylinder,' *Appl. Phys. Lett.*, **82**, pp 4379-4381, 2003.
8. J. Lagarde, O. Abraham, L. Laguerre, P.Cote, J-P Piguet, C. Balland, G. Armand, 'Use of surface waves and seismic refraction for the inspection of circular concrete structures'. *Cement & Concrete Composites*, **28**, pp 337–34, 2006.
9. R. L. Weaver, W. Sachse, and K. Y. Kim, 'Transient elastic waves in a transversely isotropic plate,' *J. Appl. Mech.*, **63**, pp 337-346, 1996.